J. Astrophys. Astr. (December 2017) 38:63
https://doi.org/10.1007/s12036-017-9481-6

Contribution of Proton Capture Reactions to the Ascertained Abundance of Fluorine in the Evolved Stars of Globular Cluster M4, M22, 47 Tuc and NGC 6397

UPAKUL MAHANTA[1,3,*], ARUNA GOSWAMI[2], H. L. DUORAH[3] and K. DUORAH[3]

[1]Department of Physics, Bajali College, Pathsala 781 325, India.
[2]Indian Institute of Astrophysics, Koramangala, Bangalore 560 034, India.
[3]Department of Physics, Gauhati University, Guwahati 781 014, India.
*Corresponding author. E-mail: upakulmahanta@gmail.com

MS received 4 March 2017; accepted 6 June 2017; published online 27 November 2017

Abstract. The origin of the abundance pattern and also the (anti)correlation present among the elements found in stars of globular clusters (GCs) remains unimproved until date. The proton-capture reactions are presently recognised in concert of the necessary candidates for that sort of observed behaviour in the second generation stars. We tend to propose a reaction network of a nuclear cycle namely carbon–nitrogen–oxygen–fluorine (CNOF) at evolved stellar condition since fluorine (^{19}F) is one such element which gets plagued by proton capture reactions. The stellar temperature thought about here ranges from 2×10^7 to 10×10^7 K and there has been an accretion occuring, with material density being 10^2 g/cm^3 and 10^3 g/cm^3. Such kind of temperature density conditions are probably going to be prevailing within the H-burning shell of evolved stars. The estimated abundances of ^{19}F are then matched with the info that has been determined for a few some metal-poor giants of GC M4, M22, 47 Tuc as well as NGC 6397. As far as the comparison between the observed and calculated abundances is concerned, it is found that the abundance of ^{19}F have shown an excellent agreement with the observed abundances with a correlation coefficent above 0.9, supporting the incidence of that nuclear cycle at the adopted temperature density conditions.

Keywords. Globular cluster—metal poor star—H-burning—abundance.

1. Introduction

The individual globular cluster gives proving grounds to models of stellar development and the investigations of their properties have added to the occasion of our present comprehension not exclusively of the galactic synthetic advancement, however likewise the progressions that the individual star have experienced over time. Maybe the primary reason that globular clusters are valuable in testing speculations of stellar development is that the stars in a specific group are thought to be contemporary, monometallic (Thévenin *et al.* 2001) old and obviously equidistant (Marcolini *et al.* 2009). However this thought has been changed since late spectroscopic reviews have uncovered that a comparable sort of wealth oddities is available even in stars that are below and above the main sequence turn-off (Decressin *et al.* 2007). Also recent observational studies have revealed star-to-star abundance inhomogeneity among light elements of stars on the main sequence in the Galactic GCs. The existence of multiple populations have recommended that these square measures also owe to some kind of 'self-pollution' (Bekki & Masashi 2007) schemes. Also GC ω Cen which is the most massive cluster, whose stars have been found to show a large spread in metallicity thereby throwing out the earlier paradigm that GCs are examples of 'Simple Stellar Populations'(SSP) (D'Ercole *et al.* 2008).

There are about 180 estimated globular clusters in and around our galaxy, some 150 of them are visible while the remainder are obscured by the galactic bulge (Ashman & Zepf 1998), among which GC M4 is closest to us and thereby making it easier to observe. Observation performed by several teams of indivisuals using high spectral resolution techniques, the GC M4 is found to be mildly metal poor with a cluster average

metallicity of $\langle[Fe/H]\rangle = -1.18$ (Ivans *et al.* 1999). Then it is conjointly peculiar owing to the fact that the CMDs have revealed that the GC M4 possesses broadened red giant branches (Marino *et al.* 2008). On the other hand GC M22 have shown a metallicity unfold and a sophisticated chemical enrichment. Moreover M22 is among the most massive galactic globular clusters and its colour-magnitude diagram (CMD) and chemical abundances have revealed the existence of sub-populations (Alves-Brito *et al.* 2012). It has been also confirmed at infrared wavelengths that this GC span a metallicity range of $-1.87 \leq [Fe/H] \leq -1.44$ thus representing a wide [Fe/H] spread (Alves-Brito *et al.* 2012). The 47 Tuc also known as NGC 104 is relatively a metal rich GC with cluster metallicity $[Fe/H] = -0.75$ is also known for its multiple populations along with a bimodal distribution of the CN bands among the giants (Ventura *et al.* 2014). NGC 6397 is the second closest GC next to M4 and is very metal-poor $[Fe/H] = -1.99$ (de Laverny & Recio-Blanco 2013) also possesses distinct bimodality and the cluster is dominated by mainly second generation stars (Lind *et al.* 2011) in which the elements are produced by mainly proton capture reactions (Ventura *et al.* 2014).

But the common thing found in these four GCs is the presence of iron peak elements (Ni, Cr, Zn), neutron capture elements (Ba, Eu, La) and α-elements (Si, Ca) (Brown & Wallerstein 1992; Gratton *et al.* 2014; Lind *et al.* 2011). Moreover different groups of people also have found that these clusters also possess CNO elements along with light odd Z elements like Na and Al (Brown & Wallerstein 1992, Alves-Brito *et al.* 2012). Moreover many observations have confirmed that there has been conjointly some correlations and anticorrelations in light elements (e.g., C, N, O, Na, Mg and Al) of stars within GCs which may offer vital clues for the early formation histories of GCs (Gratton *et al.* 2004).

However, the presence of ^{19}F which has been confirmed by observation is of the essence in all the four GCs namely M4 (Smith *et al.* 2005; Sánchez-Blázquez *et al.* 2012), M 22 (Alves-Brito *et al.* 2012, D'Orazi *et al.* 2013), NGC 6397 and 47 Tuc (de Laverny and Recio-Blanco 2013) as well. Recently (Abia *et al.* 2010) have even confirmed the presence of ^{19}F in galactic AGB stars. This ^{19}F is an interesting element of the periodic table because of the fact that though it is surrounded by some of the most abundant elements in the universe like oxygen, nitrogen and neon, after hydrogen and helium, it is itself very rare. Perhaps it is because an odd Z element with only one single stable isotope and it is very fragile with its 9 protons and 10 neutrons (Palacois 2006). However the origin of ^{19}F is still a matter of debate. The three proposed primary astrophysical factories for ^{19}F production have been the Type II supernovae (SNe II), the Wolf–Rayet (WR) stars, and the asymptotic giant branch (AGB) stars (Renda *et al.* 2004, Recio-Blanco *et al.* 2012). Each of them has different ^{19}F synthesizing mode. SNe II produces ^{19}F primarily as the result of spallation of ^{20}Ne by ν_μ and ν_τs near the collapsed core. In WR stars ^{19}F production is tied to the nuclear burning chain given by $^{14}N(\alpha,\gamma)^{18}F(\beta^+)^{18}O(p,\alpha)^{15}N(\alpha,\gamma)^{19}F$ (Lucatello *et al.* 2011). In the case of AGB stars, the reaction network $^{14}N(n,p)^{14}C(\alpha,\gamma)^{18}O(p,\alpha)^{15}N(\alpha,\gamma)^{19}F$ where the neutrons are provided by $^{13}C(\alpha,n)^{16}O$ and the protons mainly by $^{14}N(n,p)^{14}C$, i.e., it is the combination of H and He-burning in the case of AGB stars that produces ^{19}F (Renda *et al.* 2004; Lucatello *et al.* 2011). Whatever be the synthesizing process, the principles of nuclear-astrophysics are the key for understanding the presence of this element in these GC stars or galactic stars. The thermonuclear burning phases, not solely facilitate the star to achieve each thermal and hydrostatic equilibrium but additionally liable for the synthesis of various elements. However it is the temperature and density of the star which can confirm what variety of burning mode can happen within the stellar interior and the way quick burning mode will proceed. One such thermonuclear H-burning scheme that plays an important role in the abundance of elements in the surface layers of stars is the CNO cycle. This CNO cycle is answerable for manufacturing all the stable isotopes of carbon, nitrogen and oxygen. However we have chosen an extended burning mode, the CNOF cycle, which leads us to get to the element ^{19}F. In fact, the aim of this paper is to enhance our understanding and additionally to appear for brand spanking new mechanisms of fluorine production in the GC stars.

The paper is structured as follows. In section 2, we present a particular physical state of affair of the stellar environment. Section 3 presents the reactions concerned within the cycle together with the calculated values of the lifetimes for the various proton capture reaction. The evolution of ^{19}F within the cycle at equilibrium condition and the abundance of it are made public in section 4. Section 5 summarizes the discussion and a few closing remarks.

2. The stellar situation

The stellar evolution focuses on the dominant role of various stages of nuclear burning in the stellar core. Not only the temperature is crucial in any stellar situations

but density also plays an important role. Even though the density ranges from many orders of magnitude, its response in the burning rates is only linear and hence its importance is less significant as far as the elemental synthesis is concerned unless one considers a situation where low temperature and high density is prevailing. In the canonical model of the star, where the stars are assumed to be spherically symmetric, with no magnetic field, no rotation and no mass loss from the surface, the materials which are synthesized in the inner regions near the core are brought to the surface by means of convection, which is the only mixing mechanism and the convective regions are always fully mixed (Salaris *et al.* 2009). In evolved stars there are also some dredging up episodes which effectively work as far as alteration of elements is concerned. But in case of RGB star canonical extra mixing will not change the surface abundances unless it switches to an enhanced mode. This could result from tidal spin-up of upper RGB stars in close binaries (Denissenkov *et al.* 2006). Another possibility is that canonical extra mixing gets enhanced toward the RGB tip due to some internal physical processes in single stars. Another possibility is that canonical extra mixing gets enhanced toward the RGB tip due to some internal physical processes in a single star, in which the extra mixing in upper RGB stars can penetrate the H burning shell and may trigger further burning to the primary sources like ^{14}N and ^{13}C and ^{16}O along with ^{12}C. This can then be added to make the total sum of C + N + O is constant to high accuracy for stars (Smith *et al.* 2005) to yield the observed abundance of ^{19}F. Here the ^{12}C is a result of partial He burning in the He-rich intershell (Lugaro *et al.* 2004). Moreover, the proton mixing (by a process called 'partial mixing' (Casisi *et al.* 2002) in the He-rich intershell is also necessary to activate the s-process in those stars (Mowlavi *et al.* 1998). However we do not comment on the physical factors that influence the mixing or dredging up mechanisms.

3. Nuclear transformations in the CNOF cycle governing fluorine production

If heavier elements are present in some stellar conditions where the temperature is high and the density is low, then ^{12}C$(p,\gamma)^{13}$N reaction can compete with $p-p$ reaction and thereby can initiate the CNO burning mechanism (Clayton 1983 and references therein). ^{13}N is β unstable and decays to ^{13}C in a time scale of 862.77 s (Audi *et al.* 2003) since its proton capture lifetime is quite large in the considered temperature density condition. On the other hand ^{13}C is a stable isotope of carbon with relative abundance 1.1078 (Lodders 2003). This ^{13}C forms ^{14}N by taking a proton and then ^{14}N to ^{15}O taking a proton again.

Table 1. The branching ratio ($B_r = \frac{N_A\langle\sigma v\rangle_{p,\gamma}}{N_A\langle\sigma v\rangle_{p,\alpha}}$) at various temperatures in units of T_9. The rate constants for ^{15}N are taken from NACRE compilation and for ^{17}O are taken from (Iliadis *et al.* 2010).

T_9	^{15}N(B_{r1})	^{17}O(B_{r2})
0.02	4.615×10^{-4}	1.312×10^{-1}
0.03	4.232×10^{-4}	5.601×10^{-3}
0.05	3.652×10^{-4}	4.031×10^{-3}
0.08	3.134×10^{-4}	5.745×10^{-3}
0.1	2.857×10^{-4}	7.722×10^{-3}

^{14}N$(p,\gamma)^{15}$O: The experiment performed by the LUNA collaboration (Cristallo *et al.* 2014 and references therein) has reached the lowest energy, about 70 keV, which corresponds to a stellar temperature of about $T_9 = 0.05$ K. However the uncertainty on data at high energy affects the low energy extrapolation. Here we have used the rate constant values given by the NACRE compilation corresponding to our temperatures. The ^{15}O then decays via a β emission to ^{15}N in an average lifetime of 176.39 s (Audi *et al.* 2003) as ^{15}N branching appears. The branching ratio will guide how much of ^{15}N will go to form ^{16}O by taking a proton. Table 1 shows the branching ratios of the cycle at various temperatures. These branching ratios show that the (p,α) reaction wins over the (p,γ) reaction and thus confirming the cyclic behaviour forming ^{12}C by most of ^{15}N nuclei. This is the CN cycling.

^{15}N$(p,\alpha)^{12}$C: The reaction rate of this process, at the temperatures of interest for this study, is mostly determined by a resonance at $E_{cm} \sim 100$ keV. A decade ago, this reaction has been investigated using the indirect approach of the Trojan Horse Method (THM) (La Cognata *et al.* 2007), yielding results similar to (Redder *et al.* 1982). For the present work we use the reaction rate reported in the NACRE compilation. The uncertainty at relevant temperatures is about 10%.

^{15}N$(p,\gamma)^{16}$O: The low energy cross section of this process is determined by the presence of two broad resonances and by their interference. La Cognata *et al.* (2009) suggested a cross section significantly lower than the previously estimated. This translates into a significantly lower rate at AGB temperatures. In the present work we use the rate presented in NACRE compilation,

and the corresponding uncertainty at relevant temperatures is about 10%.

$^{16}O(p,\gamma)^{17}F$: This reaction was given much emphasis on the stellar temperature range of $0.06 \leq T_9 \leq 0.1$ which is important for hot bottom burning in asymptotic giant branch (AGB) stars. However the two resonances at $E_{cm} = 2.50$ and 3.26 MeV (Tilley 1993) are negligible for the total rate. The reaction rates, including uncertainties, are adopted from Iliadis *et al.* (2010) with reaction rate errors of about 7% over the entire temperature region of astrophysical interest ($T_9 = 0.01-2.5$ K).

$^{17}O(p,\alpha)^{14}N$: The reaction rate determination for this reaction, at the astrophysically relevant energy is relatively difficult and the uncertainty is correspondingly large due to the presence of the $E_{cm} = 65$ keV resonance. For the present work we adopt the value suggested by Iliadis *et al.* (2010). The uncertainty at relevant temperatures is about 20%.

$^{17}O(p,\gamma)^{18}F$: The cross section of this reaction below $E_{cm} \approx 400$ keV is determined by 2 narrow resonances. Chafa *et al.* (2007) and Newton *et al.* (2010) have determined the reaction rate with improving precision. Nevertheless, at the temperatures relevant for AGB nucleosynthesis, the reaction rate is dominated by the lowest energy resonance, $E_{cm} = 65$ keV, that is too weak to be directly measured with the current experiment possibilities. For the present work we use the reaction rate determination by Iliadis *et al.* (2010). This point onwards we take the reaction steps given in Hansen *et al.* (2004) and Mountford (2013), i.e., $^{18}O(p,\gamma)^{19}F$.

$^{18}O(p,\gamma)^{19}F$: In this case the presence of several low energy states influences the determination of the cross section. In particular, the $E_{cm} = 150$ keV broad resonance and the direct capture dominate the reaction rate at the astrophysically relevant temperature for AGB nucleosynthesis. For the present work, we adopt the reaction rate given in the recent compilation by Iliadis *et al.* (2010). The uncertainty at relevant temperatures is about 10%. Sometime the radiative capture on ^{18}O cannot be neglected as compared to $O^{18}(p,\alpha)N^{15}$ even though the (p,α) channel is substantially stronger than (p,γ) channels. Because, depending upon the spin and energy of resonance the latter can be of comparable strength (Weischer 1980). Still we have checked for possible alteration of abundances of oxygen by including a third branching point at ^{18}O. But still it does not lead us to find any significant change in the mass fraction of ^{16}O which has been found to be consistent with the earlier report of Audouze 1976 where the author had mentioned that the $^{18}O(p,\gamma)^{19}F$ leak has little effect on CNO equilibrium abundance. For instance the ^{16}O abundance changes by 12% only at temperatures $T_9 = 0.03$ and 0.05. Moreover the goal of this choice is because it may improve our knowledge of levels in the ^{19}F nucleus that are relevant to nuclear astrophysics and hopefully for a possible fluorine production network. Recently Buckner *et al.* (2012) had studied $^{18}O(p,\gamma)^{19}F$ and have found that most ^{19}F levels decay by $\gamma\gamma$-cascades through the first (110 keV) excited state, and all ^{19}F levels (with known decay schemes) de-excite through the second (197 keV) excited state. Moreover it is an interesting element in the periodic table because of the fact that though it is surrounded by some of the most abundant elements in the universe like oxygen, nitrogen and neon, it is itself very rare. Perhaps it is because of an odd Z element with only one single stable isotope and it is very fragile with its 9 protons and 10 neutrons (Palacois 2006).

$^{19}F(p,\alpha)^{16}O$: Then the finally produced ^{19}F which is destroyed by a (p,α) reaction forming ^{16}O since (p,α) reaction rate is faster as compared to (p,γ) reaction which would have produced ^{20}Ne. However (p,α) situation contains branching. Thus despite its importance, the branching ratio between α_0, α_π and α_γ outgoing channels in the $^{19}F(p,\alpha)^{16}O$ reaction are still largely uncertain at astrophysical energies, pointing out the need for new, more comprehensive, measurements. The most recent experimental work on this subject performed by La Cognata *et al.* (2011) suggested that at the lowermost energies ($T_9 < 0.1$ K), the α_0 channel dominates in the other open reaction channels (i.e. α_π and α_γ). Moreover, the presence of very low energy resonance at $E_{cm} = 300$ keV, which was not observed that before in direct measurement, until La Cognata *et al.* (2011) observed that this in an indirect experiment using the THM corresponding to typical AGB temperatures, thus implying a significant increase in the reaction rate. For example at temperatures up to $T_9 \sim 0.05$, where the reaction rate is 27% higher than in NACRE which even increases upto a factor of 1.7 ($T_9 \sim 0.1$). In this work we have compared both the reaction rates from NACRE compilation and La Cognata *et al.* (2011) and have looked for the extent up to which the ^{19}F abundance alteration has taken place. As far as the realistic astrophysical situation is concerned the reaction rate constants taken here confirm to the conditions encountered in red giants, AGB stars, classical novae, massive stars and type I X-ray bursts (Iliadis *et al.*

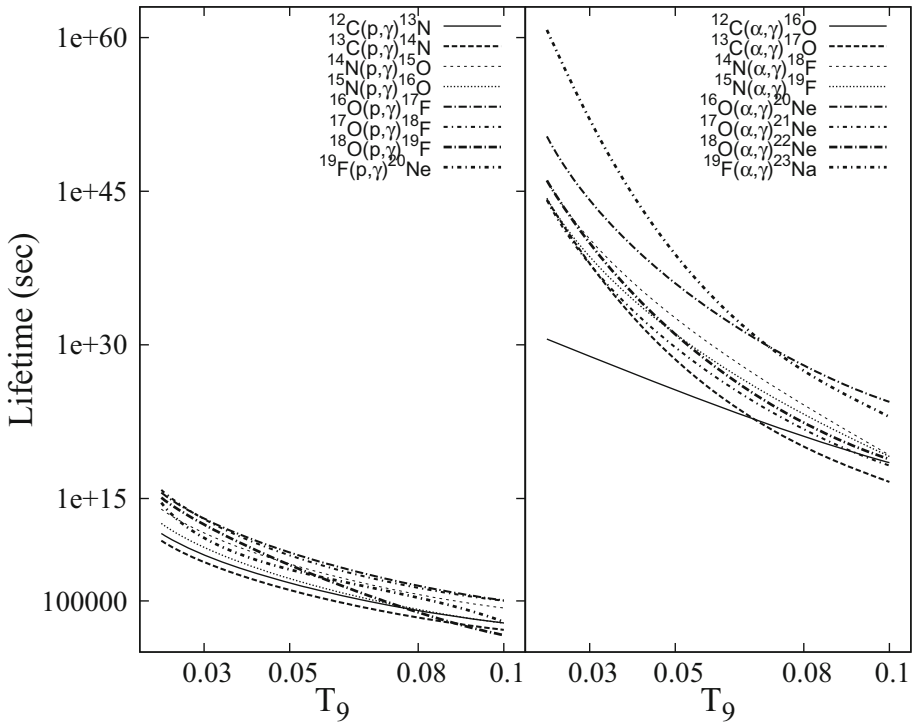

Figure 1. This figure shows a comparison of lifetimes between (p, γ) and (α, γ) reactions for all the stable nuclei present in the cycle. We notice that the (α, γ) reactions have lifetimes greater than billion years.

2010) and the same from the NACRE compilation comply with the non-explosive H- and He-burning modes with the extrapolation of astrophysical S-factors to very low energies based on potential models (Xu *et al.* 2013). Thus the CNOF cycle is as follows:

$$
\begin{aligned}
^{12}\mathrm{C} + p &\longrightarrow {}^{13}\mathrm{N} + \gamma \\
^{13}\mathrm{N} &\longrightarrow {}^{13}\mathrm{C} + e^{+} + \nu_e \\
^{13}\mathrm{C} + p &\longrightarrow {}^{14}\mathrm{N} + \gamma \\
^{14}\mathrm{N} + p &\longrightarrow {}^{15}\mathrm{O} + \gamma \\
^{15}\mathrm{O} &\longrightarrow {}^{15}\mathrm{N} + e^{+} + \nu_e \\
^{15}\mathrm{N} + p &\longrightarrow {}^{12}\mathrm{C} + \alpha \\
^{15}\mathrm{N} + p &\longrightarrow {}^{16}\mathrm{O} + \gamma \\
^{16}\mathrm{O} + p &\longrightarrow {}^{17}\mathrm{F} + \gamma \\
^{17}\mathrm{F} &\longrightarrow {}^{17}\mathrm{O} + e^{+} + \nu_e \\
^{17}\mathrm{O} + p &\longrightarrow {}^{14}\mathrm{N} + \alpha \\
^{17}\mathrm{O} + p &\longrightarrow {}^{18}\mathrm{F} + \gamma \\
^{18}\mathrm{F} &\longrightarrow {}^{18}\mathrm{O} + e^{+} + \nu_e \\
^{18}\mathrm{O} + p &\longrightarrow {}^{19}\mathrm{F} + \gamma \\
^{19}\mathrm{F} + p &\longrightarrow {}^{16}\mathrm{O} + \alpha.
\end{aligned}
$$

3.1 *Lifetime of hydrogen burning*

The rate of nuclear reactions is dependent on the density of the reactants, the velocity of one reactant relative to another, and the probability of a reaction occurring. Mathematically

$$R = \frac{1}{1+\delta_{ij}} N_i N_j \langle \sigma v \rangle, \tag{1}$$

where i, j are two separate species and δ_{ij} is the function preventing the double counting of those two species. The number density N_i of any element with mass number A_i can be converted into corresponding mass fraction X_is for the same element, for computational simplification by

$$N_i = \frac{\rho X_i N_\mathrm{A}}{A_i}. \tag{2}$$

Here ρ is the stellar density, N_A is Avogadro's number. Using this, the nuclear reaction rate of a proton capture reaction, takes the form

$$R = \frac{\rho^2 N_\mathrm{A}}{A_p A_\mathrm{he}} \left[X_p X_\mathrm{he} (N_\mathrm{A} \langle \sigma v \rangle) \right] \quad \mathrm{cm}^{-3}\,\mathrm{s}^{-1}. \tag{3}$$

Here, $N_\mathrm{A}\langle \sigma v \rangle$ is the reaction rate constant and X_he is the mass fraction of any other heavy element. The lifetime against the proton capture for the elements at the two different values of densities, has been calculated using the equation

$$\tau_p = \frac{1}{\rho X_p [N_A \langle \sigma v \rangle]} \quad \text{s.} \tag{4}$$

Here the required reaction rate constants are taken from (Iliadis *et al.* 2010) which are the recommended medium rate constant values. The $^{12}C(p,\gamma)^{13}N$, $^{13}C(p,\gamma)^{14}N$, $^{13}N(p,\gamma)^{14}O$, $^{14}N(p,\gamma)^{15}O$, $^{15}N(p,\gamma)^{16}O$, $^{15}N(p,\alpha)^{12}C$, $^{15}O(p,\gamma)^{16}F$ and the last $^{19}F(p,\alpha)^{16}O$ are also the recommended medium rate constants values which have been taken from NACRE compilation. Table 2 shows the calculated values for proton capture lifetimes for various elements in the stellar condition along with the parent nuclei's lifetime against β-decay.

There is also production of α-particles taking place in the cycle. Although it looks at first sight that these α particles may also get involved in some (α,γ) type of reactions which can lead to additional branching points in the reaction networks creating some alteration in the abundance profile of the elements. We have calculated the α-capture lifetimes for all the stable elements using an equation similar to equation (4) where X_p has been replaced by X_{He}. The rate constants for $^{12}C(\alpha,\gamma)^{16}O$, $^{13}C(\alpha,\gamma)^{17}O$, $^{14}N(\alpha,\gamma)^{18}F$, $^{15}N(\alpha,\gamma)^{19}F$, $^{16}O(\alpha,\gamma)^{20}Ne$, $^{17}O(\alpha,\gamma)^{21}Ne$, $^{18}O(\alpha,\gamma)^{22}Ne$, $^{19}F(\alpha,\gamma)^{23}Na$ reactions are taken from NACRE compilation. The estimated values of the α-capture are shown in the Table 3. Then there is also some possibilities of (α,p) type reactions mainly by the nuclei ^{14}O and ^{18}F where the former goes to ^{17}F and the later goes to ^{21}Ne. However these possibilities can also be safely ignored as the α-capture lifetimes still remain large enough even at $T_9 = 0.1$. For instance, $^{14}O(\alpha,p)^{17}F$ has a median rate constant due to NACRE compilation of magnitude 8.818×10^{-22} cm^{-3}mol^{-1} s^{-1} which gives a lifetime of 1.62×10^{19} s according to equation (4). For $^{18}F(\alpha,p)^{21}Ne$ also we find a lifetime of 4.324×10^{19} s corresponding to a rate constant 3.304×10^{-22} cm^{-3}mol^{-1}s^{-1} at $T_9 = 0.1$. We noticed that these α-capture lifetimes are much larger than the typical GC lifetime which is in the order of billion years. For instance, a recent work by a group of people (Hansen *et al.* 2013) have shown that the age of 47 Tuc is 9.7 ± 0.4 Gyr ($\approx 3.15 \times 10^{17}$ s) and the age of NGC 6397 is 11.7 ± 0.3 Gyr ($\approx 4 \times 10^{17}$ s) which is still smaller than many α-capture reactions even at $T_9 = 0.1$. Thus the possibility of α-capture can safely be ignored in the calculation, in the adopted range of temperature. Figure 1 shows a comparative view of p-capture and α-capture lifetimes for the elements involved in the cycle.

Table 2. Proton capture lifetimes τ_p (s) for various nuclear reactions. ρ_2 is the density in units 10^2 g/cm^3. Here we have shown the lifetime only for $\rho_2 = 1$ g/cm^3. For $\rho_2 = 10$ g/cm^3 the values are just only 10 times less than these values.

Reaction	T_9	$N_A\langle\sigma v\rangle$	τ_β	$\tau_p(\rho_2 = 1)$
$^{12}C(p,\gamma)^{13}N$	0.02	3.76×10^{-14}	stable	3.79×10^{11}
	0.03	1.74×10^{-11}		8.21×10^{8}
	0.05	1.31×10^{-8}		1.09×10^{6}
	0.08	2.28×10^{-6}		6.26×10^{3}
	0.1	2.03×10^{-5}		7.03×10^{2}
$^{13}C(p,\gamma)^{14}N$	0.02	1.89×10^{-13}	stable	7.55×10^{10}
	0.03	8.77×10^{-11}		1.62×10^{8}
	0.05	6.49×10^{-8}		2.20×10^{5}
	0.08	1.10×10^{-5}		1.29×10^{3}
	0.1	9.60×10^{-5}		1.48×10^{2}
$^{13}N(p,\gamma)^{14}O$	0.02	4.11×10^{-16}	862.77	3.47×10^{13}
	0.03	3.85×10^{-13}		3.71×10^{10}
	0.05	6.15×10^{-9}		2.32×10^{5}
	0.08	1.93×10^{-7}		7.40×10^{4}
	0.1	2.19×10^{-5}		6.52×10^{2}
$^{14}N(p,\gamma)^{15}O$	0.02	1.59×10^{-16}	stable	8.98×10^{13}
	0.03	1.45×10^{-13}		9.85×10^{10}
	0.05	2.21×10^{-10}		6.46×10^{7}
	0.08	6.50×10^{-8}		2.19×10^{5}
	0.1	7.20×10^{-7}		1.98×10^{4}
$^{15}N(p,\gamma)^{16}O$	0.02	3.90×10^{-15}	stable	3.66×10^{12}
	0.03	3.70×10^{-12}		3.86×10^{9}
	0.05	5.97×10^{-9}		2.39×10^{6}
	0.08	1.89×10^{-6}		7.55×10^{3}
	0.1	2.16×10^{-5}		6.61×10^{2}
$^{15}O(p,\gamma)^{16}F$	0.02	5.45×10^{-47}	176.39	2.62×10^{44}
	0.03	1.25×10^{-43}		1.14×10^{41}
	0.05	6.66×10^{-37}		2.14×10^{34}
	0.08	1.34×10^{-34}		1.06×10^{32}
	0.1	4.64×10^{-33}		3.07×10^{30}
$^{16}O(p,\gamma)^{17}F$	0.02	3.78×10^{-18}	stable	3.77×10^{15}
	0.03	6.59×10^{-15}		2.16×10^{12}
	0.05	1.98×10^{-11}		7.21×10^{8}
	0.08	9.71×10^{-9}		1.47×10^{6}
	0.1	1.30×10^{-7}		1.09×10^{6}
$^{17}F(p,\gamma)^{18}Ne$	0.02	6.12×10^{-21}	93.059	2.33×10^{18}
	0.03	2.15×10^{-17}		6.64×10^{14}
	0.05	1.36×10^{-13}		1.05×10^{11}
	0.08	1.24×10^{-10}		1.15×10^{8}
	0.1	2.17×10^{-9}		6.58×10^{6}
$^{17}O(p,\gamma)^{18}F$	0.02	2.08×10^{-18}	stable	6.86×10^{15}
	0.03	9.69×10^{-15}		1.47×10^{12}
	0.05	7.62×10^{-11}		1.87×10^{8}
	0.08	1.58×10^{-8}		9.04×10^{5}
	0.1	1.39×10^{-7}		1.02×10^{5}

Table 2. *Continued.*

Reaction	T_9	$N_A\langle\sigma v\rangle$	τ_β	$\tau_p(\rho_2 = 1)$
$^{18}F(p,\gamma)^{19}Ne$	0.02	5.47×10^{-17}	9504	2.61×10^{14}
	0.03	6.84×10^{-14}		2.08×10^{11}
	0.05	2.57×10^{-11}		5.55×10^{8}
	0.08	3.88×10^{-9}		3.68×10^{6}
	0.1	3.93×10^{-8}		3.63×10^{3}
$^{18}O(p,\gamma)^{19}F$	0.02	1.2×10^{-17}	stable	1.19×10^{15}
	0.03	1.79×10^{-14}		7.98×10^{11}
	0.05	1.35×10^{-10}		1.05×10^{8}
	0.08	7.11×10^{-6}		2.00×10^{3}
	0.1	3.17×10^{-4}		4.50×10^{1}
$^{19}F(p,\alpha)^{16}O$	0.02	3.76×10^{-17}	stable	3.79×10^{14}
	0.03	1.33×10^{-13}		2.07×10^{9}
	0.05	8.72×10^{-10}		1.63×10^{7}
	0.08	8.13×10^{-7}		1.76×10^{4}
	0.1	1.65×10^{-5}		8.65×10^{2}

4. Evolution of elemental abundance

In the cycle considered, the result per cycle before and after the branching is the production of one α-particle along with two ν_es and two e^+s. The initial nuclei are acting mainly as catalysts. Also the total mass and the total number of nuclei in the cycle is always conserved and also there is always consumption of hydrogen. Thus the net effect in the cycles is

$$\frac{dN_H}{dt} < 0, \quad \frac{dN_{He}}{dt} > 0. \tag{5}$$

The generalised differential equation that governs the evolution of any element in terms of number density via proton capture reaction or β-decay or both without any branching point is given by (Clayton 1983)

$$\dot{N}_i = -N_i N_p \langle\sigma v\rangle_{p,i} + N_j N_p \langle\sigma v\rangle_{p,j} \pm \lambda_k N_k, \tag{6}$$

where λ_k is the decay constant of the element k. As the cycle comprises of proton capture reactions and β-decays, the abundances will primarily depend upon the lifetime of these processes. If the β-decay lifetime, i.e. τ_β for an unstable element in the cycle is short as compared to its proton capture lifetime, i.e. τ, then this β-decay lifetime can be bypassed and thus the element can be thought of representing the next stable element in cycle having the same mass number, i.e. we can effectively have the β-decaying reaction which can be absorbed as ${}^{A_i}Y(p,\gamma e^+\nu_e)^{A_{i+1}}Y$, where Y is any stable isotope and A_i stands for mass number of that isotope. Considering this in equation (6) the all cycle reaction takes the form of the following differential rate equations with the branching terms as

$$\frac{d^{12}C}{dt} = -\frac{d^{12}C}{\tau_{12}} + (1 - B_{r1})\frac{d^{15}N}{\tau_{15}}, \tag{7}$$

Table 3. α capture lifetimes τ_α (s) for various nuclear reactions. ρ_2 is the density in units 10^2 g/cm^3. Here we have shown the lifetime only for $\rho_2 = 1$ g/cm^3. For $\rho_2 = 10$ g/cm^3, the values are only 10 times less than these values.

Reaction	T_9	$N_A\langle\sigma v\rangle$	$\tau_\alpha(\rho_2 = 1)$
$^{12}C(\alpha,\gamma)^{16}O$	0.02	9.86×10^{-33}	3.62×10^{30}
	0.03	4.81×10^{-31}	7.42×10^{28}
	0.05	1.20×10^{-27}	2.97×10^{25}
	0.08	7.43×10^{-23}	4.80×10^{20}
	0.1	1.15×10^{-20}	3.10×10^{18}
$^{13}C(\alpha,\gamma)^{17}O$	0.02	2.30×10^{-46}	1.55×10^{44}
	0.03	1.01×10^{-39}	3.53×10^{37}
	0.05	1.97×10^{-26}	1.81×10^{24}
	0.08	7.62×10^{-22}	4.68×10^{19}
	0.1	8.69×10^{-19}	4.11×10^{16}
$^{14}N(\alpha,\gamma)^{18}F$	0.02	3.27×10^{-48}	1.09×10^{46}
	0.03	5.51×10^{-41}	6.48×10^{38}
	0.05	3.77×10^{-33}	9.47×10^{30}
	0.08	2.77×10^{-26}	1.28×10^{24}
	0.1	2.12×10^{-21}	1.68×10^{19}
$^{15}N(\alpha,\gamma)^{19}F$	0.02	1.70×10^{-46}	2.10×10^{44}
	0.03	3.08×10^{-39}	1.16×10^{37}
	0.05	2.19×10^{-31}	1.63×10^{29}
	0.08	3.71×10^{-25}	9.62×10^{22}
	0.1	2.83×10^{-21}	1.26×10^{19}
$^{16}O(\alpha,\gamma)^{20}Ne$	0.02	1.56×10^{-52}	2.28×10^{50}
	0.03	1.32×10^{-44}	2.70×10^{42}
	0.05	4.66×10^{-36}	7.66×10^{33}
	0.08	2.11×10^{-29}	1.69×10^{27}
	0.1	1.33×10^{-26}	2.68×10^{24}
$^{17}O(\alpha,\gamma)^{21}Ne$	0.02	2.74×10^{-46}	1.30×10^{44}
	0.03	2.35×10^{-38}	1.52×10^{36}
	0.05	8.28×10^{-30}	4.31×10^{27}
	0.08	3.58×10^{-23}	9.97×10^{20}
	0.1	2.19×10^{-20}	1.63×10^{18}
$^{18}O(\alpha,\gamma)^{22}Ne$	0.02	3.22×10^{-48}	1.10×10^{46}
	0.03	2.89×10^{-41}	1.23×10^{39}
	0.05	4.49×10^{-30}	7.95×10^{27}
	0.08	8.84×10^{-24}	4.04×10^{21}
	0.1	5.25×10^{-21}	6.80×10^{18}
$^{19}F(\alpha,\gamma)^{23}Na$	0.02	6.32×10^{-63}	5.65×10^{60}
	0.03	5.96×10^{-54}	5.99×10^{51}
	0.05	5.29×10^{-34}	6.75×10^{31}
	0.08	1.76×10^{-29}	2.02×10^{27}
	0.1	3.93×10^{-25}	9.08×10^{22}

$$\frac{d^{13}C}{dt} = \frac{d^{12}C}{\tau_{12}} - \frac{d^{13}C}{\tau_{13}}, \tag{8}$$

$$\frac{d^{14}N}{dt} = \frac{d^{13}C}{\tau_{13}} - \frac{d^{14}N}{\tau_{14}} + (1 - B_{r2})\frac{d^{17}O}{\tau_{17}}, \tag{9}$$

$$\frac{d^{15}N}{dt} = \frac{d^{14}N}{\tau_{14}} - \frac{d^{15}N}{\tau_{15}}, \tag{10}$$

$$\frac{d^{16}O}{dt} = B_{r1}\frac{d^{15}N}{\tau_{15}} - \frac{d^{16}O}{\tau_{16}} + \frac{d^{19}F}{\tau_{19}}, \tag{11}$$

$$\frac{d^{17}O}{dt} = \frac{d^{16}O}{\tau_{16}} - \frac{d^{17}O}{\tau_{17}}, \tag{12}$$

$$\frac{d^{18}O}{dt} = B_{r2}\frac{d^{17}O}{\tau_{17}} - \frac{d^{18}O}{\tau_{18}}, \tag{13}$$

$$\frac{d^{19}F}{dt} = \frac{d^{18}O}{\tau_{18}} - \frac{d^{19}F}{\tau_{19}}. \tag{14}$$

In terms of mass fraction, the time evolution of any element present in the cycle is given by the following equation:

$$\dot{X}_i = \left[-R_{p,i}X_iX_p\rho + \frac{A_i}{A_j}R_{p,j}X_jX_p\rho\right]. \tag{15}$$

R_ps are $[N_A\langle\sigma v\rangle]$ terms for respective proton capture reactions of i-th and j-th element and A_i and A_j stands for the mass number of the same two nuclei involved in the cycle. Now equation (15) can be expressed as a function of the hydrogen mass fraction to get a series of first order simultaneous linear differential equations for each cycle as

$$\frac{dX_i}{dX_p} = \frac{\left[-R_{p,i}X_i + \frac{A_i}{A_j}R_{p,j}X_j\right]}{\left[-\sum_{A_i}^{A_j}\left(\frac{1}{A_i}R_{p,i}X_i\right)\right]^{-1}}. \tag{16}$$

4.1 *Calculation of* ^{19}F *abundance*

From equation (7) as (14) after converting into the format of equation (16) which are basically nothing but eight simultaneous linear first order differential equations, then solved numerically using computer software for the cycle varying the hydrogen mass fraction to $X_H = 0.4$ to get the equilibrium mass fraction abundances of ^{19}F for five different initial conditions. We assume that the heavy elements mass fraction has been shared equally by ^{12}C and ^{16}O. Thus starting with the initial condition to be as the universal one, i.e. $X_H = 0.70$, $X_{He} = 0.28$, $X_{he}(X_C^{12} = X_{^{16}O} = 0.01) = 0.02$ such that

$$X_H + X_{He} + X_{he} = 1. \tag{17}$$

We have changed only the heavy element's mass fraction to $X_{he} = 0.01$ ($X_{^{12}C} = X_{^{16}O} = 0.005$), $X_{he} = 0.002$, ($X_{^{12}C} = X_{^{16}O} = 0.001$), $X_{he} = 0.001$ ($X_{^{12}C} = X_{^{16}O} = 0.0005$) up to $X_{he} = 0.0002$ ($X_{^{12}C} = X_{^{16}O} = 0.0001$) keeping only the hydrogen mass fraction fixed. We estimated the equilibrium abundance by mass fraction of ^{19}F which are taken up to the first significant place. These abundance patterns are plotted in Fig. 2. As far as the uncertainty in the mass fraction of ^{19}F is concerned we have calculated the same at both low and high reaction rate of the individual reactions (Iliadis *et al.* 2010) and NACRE compilation. As time passes hydrogen will be consuming more and more and it will get depleted. This alteration in hydrogen mass fraction are going to be mirrored within the abundance values of alternative significant heavy elements beside ^{19}F additionally. From Fig. 2, it is seen that the mass fraction abundance values of ^{19}F of all the five figures at a given value of X_H, increases with rise in temperature upto $T_9 \leq 0.08$. We have looked for possible alteration of ^{19}F abundance for both NACRE compilation and La Cognata *et al.* (2011). For $T_9 = 0.08$ onwards, it is seen that as T_9 rises the equilibrium abundance by mass fraction of ^{19}F gets depleted to a lower value as compared to the cases of $T_9 = 0.08$. At temparature ($T_9 \leq 0.08$), the ^{19}F abundance is not found to be deviating more the 8% for initial condition $Z \sim 5 \times 10^{-4}$. However for temperature ($T_9 \geq 0.08$) and at even lower metallicity $Z \sim 10^{-4}$ the ^{19}F abundance showed variation up to 46%. Thus it is likely that at higher values of T_9 the distribution of the elements gets shifted in such a way that the abundance of ^{19}F has shown to be such. Most likely the distribution takes place amongst the other elements in the cycle. Again $^{19}F(p,\gamma)^{20}Ne$ may also be an influencial reaction at high temperature since it can then compete with $^{19}F(p,\alpha)^{16}O$. Moreover, as stated earlier, at larger temperature the ^{19}F destruction via (p,α) reaction deviates from non-resonant to behaviour which in turn makes an increment in destruction rate of ^{19}F. Now this abundance by mass fraction of ^{19}F and the hydrogen mass fractions at which ^{19}F mass fractions are obtained are used to calculate the abundance of ^{19}F using equation (18)

$$\epsilon(^{19}F) = \log\left[\frac{N(^{19}F)}{N(H)}\right] + 12. \tag{18}$$

Table 5 shows the observed and the estimated abundances of ^{19}F for all the metal poor stars of M4 reported in Smith *et al.* (2005), M22 in Alves-Brito *et al.* (2012) and 47 Tuc along with NGC 6397 in de Laverny & Recio-Blanco (2013) along with the difference between the observed and the calculated abundances are shown in the last column for each GCs. Figure 3 shows comparative view of the tabulated values of both the calculated

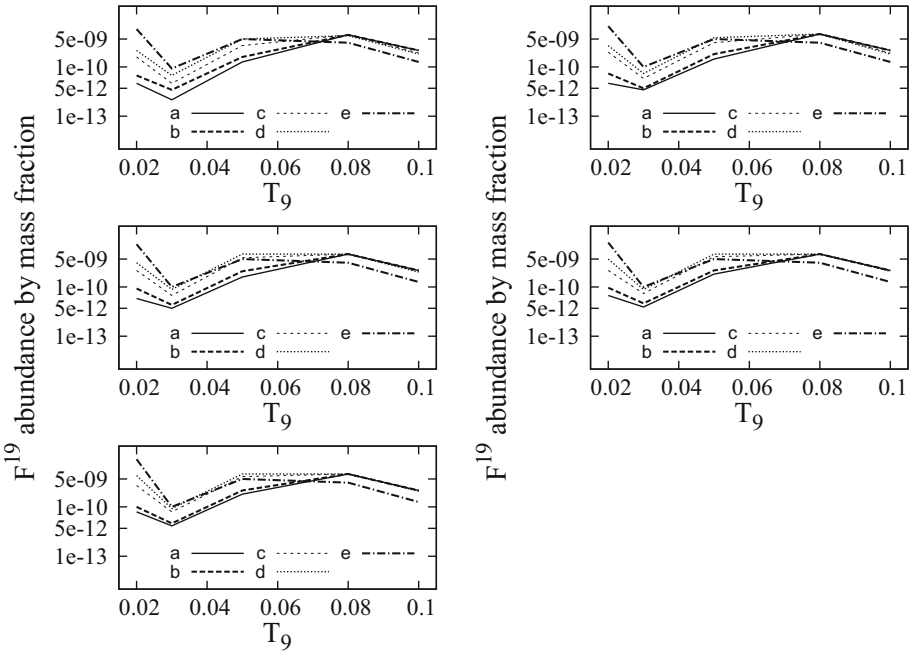

Figure 2. The ^{19}F abundance shown as a function of temperature (T_9) at different hydrogen mass fractions (*top left* at $X_{\rm H} = 0.55$, *top right* at $X_{\rm H} = 0.52$, *middle left* at $X_{\rm H} = 0.48$, *middle right* at $X_{\rm H} = 0.45$, *bottom left* at $X_{\rm H} = 0.42$) at five different initial conditions which are $a = X_{^{12}\rm C} = X_{^{16}\rm O} = 0.01$, $b = X_{^{12}\rm C} = X_{^{16}\rm O} = 0.005$, $c = X_{^{12}\rm C} = X_{^{16}\rm O} = 0.001$, $d = X_{^{12}\rm C} = X_{^{16}\rm O} = 0.0005$, $e = X_{^{12}\rm C} = X_{^{16}\rm O} = 0.0001$. The ^{19}F abundance grows as T_9 rises but after $T_9 \geq 0.08$ its abundance have shown some decrement. This may be because there are other elements present too in the cycle which abundance might have shown alteration after that temperature. Moreover at larger temperature the ^{19}F destruction via (p, α) reaction deviates from non-resonant to resonant behaviour leading to an enhanced reaction rate.

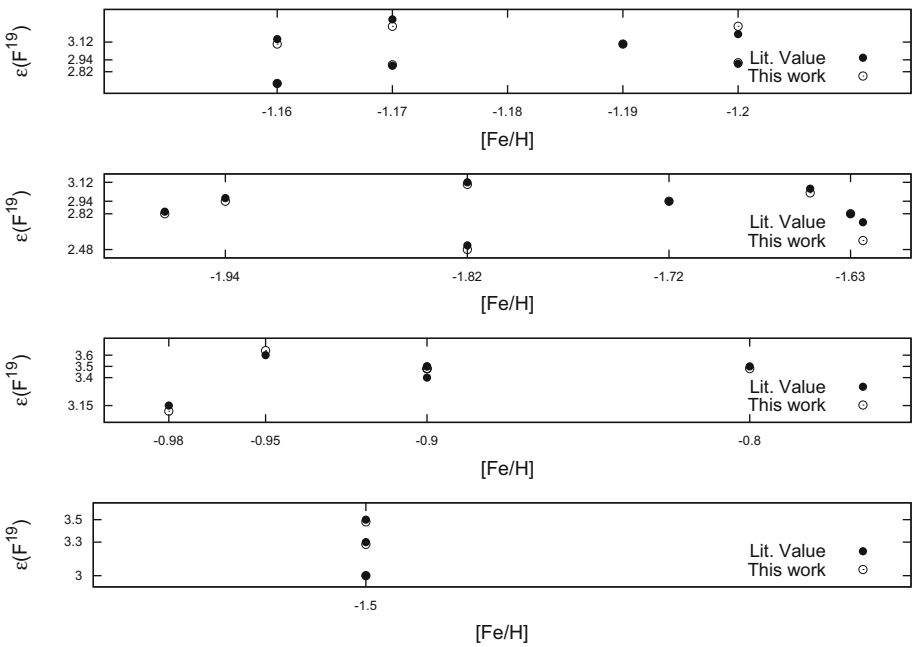

Figure 3. A comparative view of calculated and observed values of abundances of those selected stars of Table 4 is shown. The filled circles are values, obtained from literature and open cirles are the values, calculated from this work. *First panel*: GC M4 (Smith *et al.* 2005), *second panel*: GC M22 (Alves-Brito *et al.* 2012), *third panel*: 47 Tuc (de Laverny & Recio-Blanco 2013) and *fourth panel*: for NGC 6397 (de Laverny & Recio-Blanco 2013). We have plotted the $\epsilon(^{19}\rm F)$ for star III-12 and III-14 of GC M22 #68039 of 47 Tuc and all of NGC 6397 to be the maximum one as tabulated.

Table 4. The elemental abundances for ^{19}F are found at different hydrogen mass fractions with different initial heavy element's condition. $X = X_{^{12}C} = X_{^{16}O}$ and $\delta\left[\epsilon(^{19}F)\right] = \text{mod}\,[[\epsilon(^{19}F)]_{\text{Smith}} - [\epsilon(^{19}F)]_{\text{this work}}]$.

M4					
Star	$\epsilon(^{19}F)^a$	$\epsilon(^{19}F)^b$	X	T_9,ρ_2	$\delta\left[\epsilon(^{19}F)\right]$
1411	2.90	2.91	0.0001	0.03,1	0.01
1514	3.15	3.10	0.0005	0.05,1	0.05
2307	3.10	3.10	0.0005	0.05,1	0.00
3209	3.20	3.28	0.0001	0.02,1	0.08
3413	3.35	3.28	0.0001	0.02,1	0.07
4611	2.70	2.70	0.0001	0.05,1	0.00
4613	2.88	2.89	0.0005	0.05,1	0.01
M22					
Star	$\epsilon(^{19}F)^c$	$\epsilon(^{19}F)^b$	X	T_9,ρ_2	$\delta\left[\epsilon(^{19}F)\right]$
IV-97	2.97	2.94	0.001	0.05,1	0.03
IV-102	2.84	2.82	0.0001	0.03,1	0.02
III-3	2.94	2.94	0.001	0.08,1	0.00
III-12	≤ 3.06	3.02	0.0005	0.05,1	≤ 0.04
III-14	≤ 2.52	2.48	0.001	0.05,1	≤ 0.04
III-15	3.12	3.10	0.0005	0.05,1	0.02
III-52	2.82	2.82	0.0001	0.03,1	0.00
47 Tuc					
Star	$\epsilon(^{19}F)^d$	$\epsilon(^{19}F)^b$	X	T_9,ρ_2	$\delta\left[\epsilon(^{19}F)\right]$
#41806	3.15	3.10	0.0005	0.05,1	0.05
#68261	3.4	3.48	0.0001	0.02,1	0.08
#56265	3.5	3.48	0.0001	0.02,1	0.02
#68039	< 3.5	3.48	0.0001	0.02,1	< 0.02
#38841	3.5	3.48	0.0001	0.02,1	0.02
#86622	3.6	3.64	0.0001	0.02,1	0.04
NGC 6397					
Star	$\epsilon(^{19}F)^d$	$\epsilon(^{19}F)^b$	X	T_9,ρ_2	$\delta\left[\epsilon(^{19}F)\right]$
#73589	< 3.0	3.00	0.0001	0.03,1	0.00
#73212	< 3.3	3.28	0.0001	0.02,1	< 0.02
#51362	< 3.5	3.48	0.0001	0.02,1	< 0.02
#52830	< 3.7	3.64	0.0001	0.02,1	< 0.06

[a]Smith *et al.* (2005), [b]this work, [c]Alves-Brito *et al.* (2012) and [d]de Laverny and Recio-Blanco (2013).

and observed abundances of the metal poor stars of the four clusters against the respective [Fe/H] values. The [Fe/H] values used here are the [Fe$^{\text{I}}$/H] values directly taken from the respective authors except for M4. In the case of M4 the reported values of ϵ(Fe) are first converted into their respective [Fe/H] values by the equation [Fe/H] $= \epsilon(\text{Fe}) - \epsilon(\text{Fe})_\odot$ with $\epsilon(\text{Fe})_\odot = 7.45$.

4.2 Na–F *(anti-) correlation*

Although F measurements are available for only small samples of star and they exhibit star-to-star variations within the GCs, the data available for some GCs suggest a Na–F anticorrelation. The top left panel of Fig. 4 shows ^{19}F abundance both calculated and observed plotted against the observed ^{23}Na abundance reported in Smith *et al.* (2005) for GC M4 and the same reported in Alves-Brito *et al.* (2012) for GC M22 (top right panel) respectively, which shows clearly the anticorrelated behaviour between ^{19}F and ^{23}Na. Then in the bottom left panel the trend of anticorrelated behaviour between the calculated abundance of ^{19}F and the observed abundance of ^{23}Na reported in de Laverny and Recio-Blanco (2013) is also seen in NGC 6397 for considered sample size. However the same trend has not been seen between the estimated and observed abundances of ^{19}F and ^{23}Na in the selected sample of the 47 Tuc which is consistent with the report given by de Laverny and Recio-Blanco (2013). The abundance of ^{23}Na is calculated by the following equation

$$\epsilon(^{23}\text{Na}) = \left[\frac{\text{Na}}{\text{Fe}}\right] + \left[\frac{\text{Fe}}{\text{H}}\right] + 6.17. \quad (19)$$

5. Discussion and concluding remarks

The fluorine production because of the p-capture reaction has been researched utilizing refreshed reaction rates (Iliadis *et al.* 2010) and NACRE compilation for nuclear cycle CNOF in advanced stellar conditions. The ^{19}F abundance square measures figured and with their counterparts in a specimen of metal poor stars of GC M4, M22, 47 Tuc and in NGC 6397 (Fig. 3) to comprehend the degree to which this nuclear reaction cycle can clarify the observed plenitudes of fluorine. We have likewise identified some comparative sort of patterns in the fluorine abundance, in the stars of all the four GCs.

We likewise found that inside the temperature and density conditions considered, there exists a little scope of temperature qualities at which the figured $\epsilon(^{19}F)$ values coordinate with the observed values in stars of GCs M4, M22, 47 Tuc and in NGC 6397 quite well. It has been furthermore detailed in Denissenkov and Tout (2000) that temperature of H-burning shell in red giants never surpasses on the far side of $T_9 = 0.055$ that is keeping our calculation aside from the GC M4.

Moreover in Fig. 4 the estimated ^{19}F abundance is seen clearly in an anticorrelation with the ^{23}Na abundance for all of the clusters as so much as these

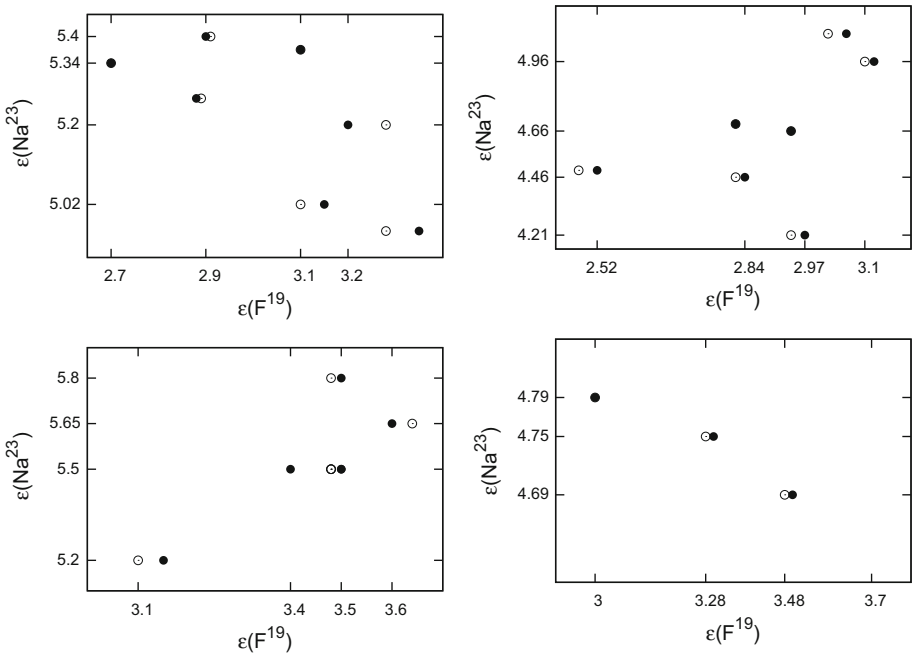

Figure 4. The signs of (anti)correlation between ^{19}F and ^{23}Na are shown. The filled circles are values obtained from literature and open cirles are the values, calculated from this work. *Top left panel*: GC M4. The calculated values of ^{19}F are taken from this work and ^{23}Na which are the observed values of abundances are taken from Smith *et al.* (2005). *Top right panel*: GC M22. Here also the calculated values of ^{19}F are taken from this work and the observed values of ^{23}Na are taken from Alves-Brito *et al.* (2012). *Bottom left panel*: NGC 6397 and *bottom right panel*: 47 Tuc, where the observed abundances for ^{23}Na are taken from de Laverny & Recio-Blanco (2013).

samples are concerned except for 47 Tuc. The elements formed following proton-capture synthesis may have been brought to the surface by dredge-up mechanisms (Salaris *et al.* 2002; Karakas 2010). It has also been reported in Denissenkov and Tout (2000), that the Zahn's mechanism which is believed to be a result of the joint operation of meridional circulation and turbulent diffusion, could be an efficient process to bring the synthesized material to the stellar surface. This mechanism operates in the radiative zone separating the hydrogen-burning shell and the base of the convective envelope (Denissenkov and Tout 2000). The shear mixing and the horizontal turbulence are also important agents for effective transport of chemical elements and angular momentum since low metallicity the rotational mixing plays a dominant role (Meynet 2008). As the materials are carried to the surface which carry angular momentum with them, the stars get their rotational motion. Once the rotational speed reaches the critical value the stars start to lose their mass in the form of these synthesized materials in the outer space thus enriching the space by these materials or which may be trapped by other stars by accretion if they are already present. Thus mixing and mass-loss that are also acknowledged to have an effect on the elemental abundances. For instance a mass loss rate of 10^{-13} $M_{\odot}$ yr^{-1} reduces both internal and surface anomalies by up to a factor of 6–7. Then for a mass loss rate of 10^{-12} $M_{\odot}$ yr^{-1} anomalies reduce to below 0.2 dex. Also the same mass loss can lead to generalized under abundances for all elements, lower mass loss rates enable over abundances to develop on the surface (Vick *et al.* 2013).

It would also be interesting to check the effect of certain beta decay lifetimes which may change under certain temperature-density conditions leading to the change in the lifetimes of the nuclear cycle and thereby creating alteration in the calculated abundance profile (Goswami *et al.* 1992 and references therein). Moreover, the affect of resonance in nuclear reactions which can change the rate of the reaction which in turn can effect the abundance profiles of elements has not been addressed here either, although it is important to note that some of the reactions in these cycles may be resonating. Moreover we have considered the cyclic behaviour of reaction networks, i.e. the evolution of elements are confined. However there may also be some leakage of ^{19}F going to ^{20}Ne via a proton-capture reaction. Moreover at high temparature ^{19}F(α, p)^{22}Ne reaction also gets activated which is an important reaction for fluorine destruction. The possibilities of other

internal pollution mechanisms (D'Orazi *et al.* 2013) within the cluster are also likely to affect the abundance pattern. In addition, theoretical uncertainties are likely to remain especially in the calculation of reaction rates (Iliadis *et al.* 2010), and also in the choice of the initial condition.

Nevertheless the important thing which has been observed is that the computed abundance values of ^{19}F with the present set of initial conditions do not deviate much from the observed values, gives justification to the possibility of occurrence of this cycle at those temperature density conditions which are relevant to those stellar environments.

Acknowledgements

We are grateful to Dr. Indira Bordoloi for many constructive suggestions which has improved considerably the readability of the paper. The author would also like to thank Mr. Rakesh Moulick for performing some initial computer programing while preparing the manuscript.

References

Abia, C., Cunha, K., Cristallo, S., de Laverny, P., Domínguez, I., Eriksson, K., Gialanella, L. Hinkle, K., Imbriani, G., Recio-Blanco, A., Smith, V. V., Straniero, O., Wahlin, R. 2010, *ApJL*, **715**, L94.

Alves-Brito, A., Yong, D., Meléndez, J., Vásquez, S., Karakas, I. A. 2012, *AAP*, **540**, A3.

Ashman, K. M., Zepf, S. E. 1998, in: *Globular Cluster Systems*, Cambridge University Press, Cambridge.

Audi, G., Bersillonb, O., Blachotb, J., Wapstracet, A. H., 2003, *Nucl. Phys. A*, **729**, 3–128.

Audouze, J. 1976, *CNO isotopes in astrophysics*, General Assembly, Special Session, Grenoble, France, August 30.

Bekki, K., Masashi, C. 2007, *ApJ*, **665**, 1164–1172.

Brown, J. A., Wallerstein, G. 1992, *AJ*, **104**, 1818.

Buckner, M. Q., Iliadis, C., Cesaratto, J. M., Howard, C., Clegg, T. B., Champagne, A. E., Daigle, S. 2012, *Phys. Rev.*, *C*, **86**, 065804.

Casisi, S., Salaris, M., Bono, G. 2002, *APJ*, **565**, 1231.

Chafa, A., Tatischeff, V., Aguer, P., *et al.* 2007, *Phys. Rev. C*, **75**, 035810.

Cristallo, S., Di Leva, A., Imbriani, G., Piersanti, L., Abia, C., Gialanella, L., Straniero, O. 2014, *A& A*, **570**, A46.

Clayton, D. D. 1983, in: *Principles of stellar evolution and nucleosynthesis*, University of Chicago Press, Chicago and London.

D'Ercole, A., Vesperini, E., D'Antona, F., McMillan, L. W. S., Recchi, S. 2008, *MNRAS*, **391**, 825.

Decressin, T., Meynet, G., Charbonnel, C., Prantzos, N., Ekström S. 2007, *A&A*, **464**, 1029–1044.

de Laverny, P., Recio-Blanco, A. 2013, *AAP*, **555**, A121.

Denissenkov, A. P., Tout, A. C. 2000, *MNRAS*, **316**, 395–406.

Denissenkov, P. A., Chaboyer, B., Li, K. 2006, *ApJ*, **641**, 1087.

D'Orazi, V., Lucatello, S., Lugaro, M., Gratton, R. G., Angelou, G., Bragaglia, A., Carretta, E., Alves-Brito, A., Ivans, I. I., Masseron, T., Mucciarelli, A. 2013, *ApJ*, **763**, 22.

Gratton, R., Sneden, C., Carretta, E. 2004, *ARA&A*, **42**, 385–440.

Goswami, A., Ramadurai, S., Duorah, H. L. 1992, *AP&SS*, **188**, 233.

Hansen, J. C., Kawaler, D. S., Timble, V. 2004, in: *Stellar Interiors Physical Principles, Structure and Evolution*, 2nd edition, Springer-Verlag, New York Inc.

Hansen, B., Kalirai, J. S., Anderson, J., Dotter, A., Richer, H., Rich, R., Shara, M., Fahlman, G., Hurley, J., King, I., Reitzel, D., Stetson, P. 2013, *Nature*, **500**, 51.

Iliadis, C., Longland, R., Champagne, A. E., Coc, A., Fitzgerald, R. 2010, *Nucl. Phys.*, *A*, **841** (1), 31–250.

Ivans, I. I., Sneden, C., Kraft, P. R., Suntzeff, N. B., Smith, V. V., Langer, G. E., Fulbright, J. P. 1999, *AJ*, **118**, 1273–1300.

Karakas, I. A. 2010, in: *Principles and Perspectives in Cosmochemistry*, Eds A. Goswami & B. E. Reddy, Springer, ASSP, p. 107.

La Cognata, M., Mukhamedzhanov, A. M., Spitaleri, C. *et al.* 2011, *Astrophys. J. Lett.*, **739**, L54.

La Cognata, M., Goldberg, V. Z., Mukhamedzhanov, A. M., Spitaleri, C., Tribble, R. E. 2009, *Phys. Rev. C*, **80**, 012801.

La Cognata, M., Romano, S., Spitaleri, C., *et al.* 2007, *Phys. Rev.*, *C*, **76**, 065804.

Lind, K., Charbonnel, C., Decressin, T., Primas, F., Grundahl, F., Asplund, M. 2011, *AAP*, **527**, A148.

Lodders, K. 2003, *ApJ*, **591**, 1220–1247.

Lucatello, S., Masseron, T., Johnson, J. A., Pignatari, M., Herwig, F. 2011, *ApJ*, **729**, 40 (13 pp.).

Lugaro, M., Ugalde, C., Karakas, A. I., Grres, J., Wiescher, M. *et al.* 2004, *ApJ*, **615**, 934.

Marcolini, A., Gibson, B. K., Karakas, A. I., Sánchez-Blázquez, P. 2009, *MNRAS*, **395**, 719.

Marino, A. F., Villanova, S., Piotto, G., Milone, A. P., Momany, Y., Bedin, L. R., Medling, A. M. 2008, *AAP*, **490**, 625–640.

Meynet, G. 2008, *Stellar Nucleosynthesis: 50 years after B^2FH*, edited by C. Charbonnel and J. P. Zahn, EAS Publications Series, vol. 32, pp. 187–232.

Mowlavi, N., Jorissen, A., Arnould, M. 1998, *A&A*, **334**, 153.

Mountford, D. J. 2013, Ph.D. Thesis, The University of Edinburgh.

Newton, J. R., Iliadis, C., Champagne, A. E. *et al.* 2010, *Phys. Rev. C*, **81**, 045801.

Palacois, A. 2006, *Stars and Nuclei: A Tribute to Manuel Forestini*, Eds T. Montmerle & C. Kahane, EAS Publication Series vol. 19, 67–84.

Recio-Blanco, A., de Laverny, P., Worley, C., Santos, N. C., Melo, C., Israelian, G. 2012, *AAP*, **538**, A117.

Redder, A., Becker, H. W., Lorenz-Wirzba, H. *et al*. 1982, *Zeitschrift fur Physik A Hadrons and Nuclei*, **305**, 325.

Renda, A., Fenner, Y., Gibson, K. B., Karakas, I. A., Lattanzio, C. J., Campbell S., Chieffi, A., Cunha, K., Smith V. V. 2004, *MNRAS*, **354**, 575–580.

Sánchez-Blázquez, P., Marcolini, A., Gibson, B. K., Karakas, A. I., Pilkington, K., Calura, F., 2012, *MNRAS*, **419**, 1376.

Salaris, M., Cassisi, S., Weiss, A. 2002, *PASP*, **114**: 794, 375–402.

Salaris, M., Serenelli, A., Weiss, A., Miller Bertolani, M. 2009, *APJ*, **692**, 1013.

Smith, V. V., Cunha, K., Ivans, I. I., Lattanzio, C. J., Campbell, S., Hinkle, H. K., 2005, *ApJ*, **633**, 392–397.

Thévenin, F., Charbonnel, C., Pacheco, J., de Freitas, A., Idiart, T. P., Jasniewicz, G., de Laverny, P., Plez, B. 2001, *AAP*, **373**, 905–915.

Tilley, D. R., *et al.* 1993, *Nucl. Phys. A*, **564**, 1.

Ventura, P., Di Criscienzo, M., D'Antona, F., Vesperini, E., Tailo, M., Dell'Agli, M., D'Ercole, A. 2014, *MNRAS*, **437(4)**, 3274–3282.

Vick, M., Michaud, G., Richer, J., Richard, O. 2013, *A&A*, **552**, A131.

Weischer, M. *et al.* 1980, *Nucl. Phys.*, *A*, **349**, 165.

Xu, Y., Takahashi, K., Goriely, S., M. Arnould, M., Ohta, M., Utsunomiya, H. 2013, *Nucl. Phys. A*, **918**, 61–169.